

**eDNA TRANSPORT IN STREAMS WITH COARSE
SEDIMENT BED**

by
Kush Paliwal

A Thesis

*Submitted to the Faculty of Purdue University
In Partial Fulfillment of the Requirements for the degree of*

Master of Science in Civil Engineering



Lyles School of Civil Engineering
West Lafayette, Indiana
December 2021

THE PURDUE UNIVERSITY GRADUATE SCHOOL
STATEMENT OF COMMITTEE APPROVAL

Dr. Antoine Aubeneau, Chair
Lyles School of Civil Engineering

Dr. Cary Troy
Lyles School of Civil Engineering

Dr. Zhi Zhou
Lyles School of Civil Engineering

Approved by:
Dr. Dulcy Abraham

*Dedicated to my Naani,
Late Smt. Manorama Paliwal.*

ACKNOWLEDGMENTS

This thesis was a unique learning experience to me and will not be complete without recognizing the support and assistance I have received from some people. I would first like to thank my advisor, Professor Antoine Aubeneau, whose expertise was invaluable in formulating this research. Your insightful feedback pushed me to sharpen my thinking and brought my work to a higher level. I am also grateful to my committee members, Professor Zhi Zhou and Professor Cary Troy for lending their invaluable time and knowledge to this work. I would also like to thank our lab manager William Schmidt for always being there with his lab expertise and technical assistance.

Getting through my dissertation required more than just academic support, and for that I would like to thank Shubham for supporting me and always keeping me motivated in my thick and thin. I would also like to thank Pallavi for patiently tolerating me for the past year.

Finally, and most importantly, I would like to express my gratitude to my parents and by brother, Dhruv, for believing in me and without whose tremendous support it would have been impossible for me to complete this study.

TABLE OF CONTENTS

| | |
|--|----|
| LIST OF TABLES | 6 |
| LIST OF FIGURES` | 7 |
| NOMENCLATURE | 8 |
| ABSTRACT..... | 9 |
| 1. INTRODUCTION | 10 |
| 2. METHODS | 13 |
| 2.1 Experimental Setup | 13 |
| 2.2 Conservative Tracer Experiments..... | 15 |
| 2.3 eDNA Experiments | 16 |
| 2.3.1 Retention Rate | 17 |
| 2.3.2 Breakthrough Curves | 18 |
| 2.3.3 Filtration and Extraction | 19 |
| 2.3.4 DNA Quantification..... | 20 |
| 2.4 Transport Modelling | 21 |
| 2.4.1 Retention Rates | 21 |
| 2.4.2 Transient Storage Model..... | 22 |
| 3. RESULTS | 24 |
| 3.1 Retention Rate and Breakthrough Curves..... | 24 |
| 3.2 Modeling and Transport Parameters | 26 |
| 3.3 Variability | 30 |
| 4. DISCUSSION AND CONCLUSION | 31 |
| REFERENCES | 34 |
| APPENDIX A. TABLES AND FIGURES | 38 |
| APPENDIX B. MATLAB CODES | 42 |
| APPENDIX C. R-TSM ANALYTICAL SOLUTION | 43 |
| APPENDIX D. RELATIONSHIP BETWEEN THE EFFECTIVE REACH-SCALE UPTAKE RATE AND THE ACTUAL REACTION RATE IN THE TRANSIENT ZONE | 45 |

LIST OF TABLES

| | |
|---|----|
| Table 1. Conservative tracer experiment details..... | 15 |
| Table 2 eDNA experiment details..... | 16 |
| Table 3. Genus Specific Primers used to amplify Salmo Salar DNA..... | 20 |
| Table 4. Estimated transport parameters and root mean square error (RMSE). | 29 |

LIST OF FIGURES`

| | |
|---|----|
| Figure 1. Conceptual model of the source, transport, and fate of eDNA in a stream environment. Processes illustrated here include eDNA shedding, retention, advection/dispersion, settling, and resuspension. (Created with BioRender.com). | 10 |
| Figure 2. Experimental setup. Picture of the horizontal flume (10 m long; 0.32 m wide) along with the tanks (1000 L each) used for preparing influent solutions. Tank 1 was used to supply clean water, and Tanks 2 and 3 were used for eDNA injections. A 10 cm layer of pea gravel was laid to the flume bed. The flow is from right to left..... | 13 |
| Figure 3. Schematic diagram of the experimental setup..... | 14 |
| Figure 4. eDNA quantification steps: Sampling, Filtration, Extraction, Detection (clockwise). . | 17 |
| Figure 5 Conceptual representation showing main channel and transient storage zone processes [Runkel and Broshears, 1991]. Calibration parameters in the model include main channel cross-sectional area (A), storage zone area (A_s), storage exchange coefficient (α), and dispersion coefficient (D)..... | 22 |
| Figure 6. Natural log of eDNA by distance. The solid red line is a regression fit to the data (N=15) representing the estimated retention rate ($R^2 = 0.8867$, $p = 0.016$). Each point represents the dilution corrected mean natural log transformed eDNA concentration \pm SE bars (N = 3) for each station..... | 24 |
| Figure 7. Normalized breakthrough curves of eDNA (observed and predicted) and NaCl solutions through the flume for Experiment BTC_Rep1 and BTC_Rep2. | 25 |
| Figure 8. Model results for experiment BTC_Rep2 showing the conservative tracer in blue (salt) and eDNA in green with normalized concentration on the y-axis and time (in seconds) on the x-axis. The solid red line shows the Transient Storage Model fit to the salt and the dashed red line the fit to the eDNA. Model parameter values are given in Table 4. | 26 |
| Figure 9 Model fit with a full model with free transient and reactive parameters (only advection and dispersion fixed) for experiment BTC_Rep2. Notice the log scale on the y axis. The eDNA breakthrough curve is represented perfectly by a TSM with reactions in the water column and in the bed. The exchange rate (α) between the stream and the bed is much higher for the particulate than for the solute, a measure of the settling. The reactive parameters k_m and k_{im} represent permanent removal processes (long term sorption, filtration). | 28 |
| Figure 10. Normalized breakthrough curves of eDNA (observed and predicted) and NaCl solutions through the flume for Experiment BTC_Variance. | 30 |

NOMENCLATURE

| | | |
|----------|---|---|
| A | = | stream channel cross-sectional area [m^2] |
| A_S | = | storage zone cross-sectional area [m^2] |
| C | = | in-stream solute concentration [mass/m^3] |
| C_0 | = | influent eDNA concentration [mass/m^3] |
| C_S | = | storage zone solute concentration [mass/m^3] |
| C_x | = | eDNA concentration at x m downstream from the injection site [mass/m^3] |
| D | = | dispersion coefficient [m^2/s] |
| k_{im} | = | first order removal rate constant in the storage zone [$1/\text{sec}$] |
| k_m | = | first order removal rate constant [$1/\text{sec}$] |
| k_t | = | uptake rate constant [$1/\text{sec}$] |
| k_x | = | retention rate [$1/\text{m}$] |
| Q | = | volumetric flowrate [m^3/s] |
| S | = | Slope [m/m] |
| S_w | = | uptake length [m] |
| u | = | average flow velocity (m/s) |
| α | = | mass transfer rate [$1/\text{s}$] (with the inverse expressing a timescale) |
| β | = | capacity coefficient representing the ratio of volumes of the immobile zone (sediment bed) to the mobile zone (free stream), sometimes also called A_S/A in TSM formulations (with A = stream channel cross-sectional area [m^2] and A_S = storage zone cross-sectional area [m^2]) |

ABSTRACT

Environmental DNA (eDNA) is organismal DNA found in nature. It has emerged as a practical way to measure species distribution and abundance in their habitat. Because eDNA is transported in the environment, knowing where it originates remains a challenge, particularly in flowing waters. eDNA is a heterogeneous mixture of particulate organic matter that settles out of the water column and can be trapped in or near the bed sediment. eDNA data collected during experiments or surveys have a large amount of unexplained variability, making it hard to constrain eDNA transport models. The two guiding questions we answer in this thesis are: 1) Can we predict eDNA transport patterns in a flowing system? and 2) Can we explain the observed variability in eDNA data by the interfacial processes between the water column and the sediment bed? We conducted three experiments in an artificial laboratory channel. In the first experiment, we measured eDNA retention, i.e., the distance eDNA travels downstream of an injection on average. In the second experiment, we compared the observed breakthrough behavior to the predicted pattern from the first experiment results. Finally, in the last experiment, we loaded the streambed with eDNA prior to reproducing the second experiment. For the first experiment (retention), we injected known quantities of Atlantic Salmon (*Salmo Salar*) and sampled the water column at five locations during the plateau phase. We measured the retention rate as the slope of the (logged) concentration data vs downstream distance and the travel distance as its inverse. The measured travel distance in our small channel (30 cm wide) with a coarse sediment bed (1 cm d_{50}), low flow (1 L/s) and shallow water column (10 cm) was 18.51 m (15.38 – 23.24 m, \pm SE). We used the measured retention rate to predict the breakthrough behavior with a simple transport model and showed good agreement between the predicted and the observed concentrations measured in the second experiment. The results from the third experiment had the same overall pattern, but with more variability. Our results indicate that eDNA settling out of the water column and filtration in the streambed may limit the distance eDNA travels downstream and thus constrain where it came from. We also demonstrated that exchange processes between the water-column and the bed-sediment could explain the observed variability in eDNA transport data, suggesting a crucial influence of parafluvial processes in eDNA transport.

1. INTRODUCTION

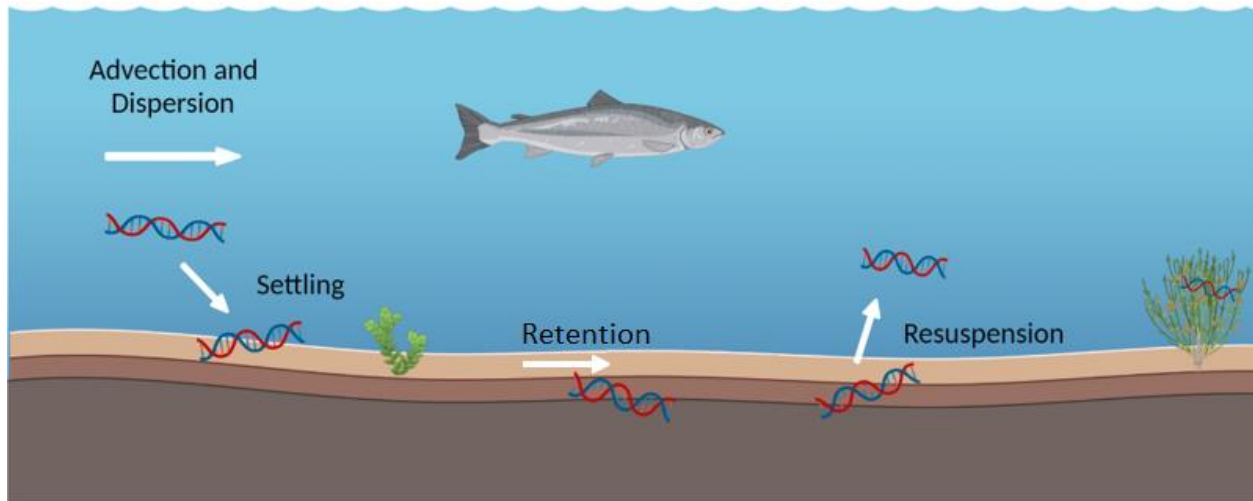


Figure 1. Conceptual model of the source, transport, and fate of eDNA in a stream environment. Processes illustrated here include eDNA shedding, retention, advection/dispersion, settling, and resuspension. (Created with BioRender.com).

Traces of genetic material abound in the environment where organisms shed cells and tissue. The DNA extracted from these biological remains is called environmental DNA (eDNA). eDNA is a highly sensitive and non-intrusive method to identify species in their habitat without observing them directly. Scientists and managers are now considering eDNA over traditional and often disruptive methods such as electrofishing or net trapping for example [Bohmann et al., 2014]. Quantitative PCR (Polymerase Chain Reaction) can detect but also quantify the genetic material, offering new ways to measure populations [Takahara et al., 2012]. eDNA has been used in various habitats including air [Johnson et al., 2019], soils [Hartvig et al., 2021] and forests [Kirse et al., 2021], but mostly in aquatic environments, where it detected endangered [Pfleger et al., 2016; Mizumoto et al., 2017], invasive [Ardura et al., 2015; Xia et al., 2017], and rare [McKelvey et al., 2015] species. eDNA has proved its potential as a novel approach to describe and understand aquatic systems.

eDNA is very effective to detect otherwise invisible species, yet a positive detection poses many questions. What if the eDNA was transported over large distances before it was sampled? In still water, Takahara et al. [2012] could relate qPCR data to carp biomass and distribution in a lagoon. However, even in standing water, eDNA could be transported by birds or fishermen and

finding eDNA may not always pinpoint the recent location of the target species [Bothwell et al., 2009]. In lotic systems, eDNA can be transported downstream and its origin difficult to track [Jane et al., 2014]. Deiner et al. [2016] used metabarcoding in a river network to identify all possible eucaryotic families. They showed that many terrestrials species were detected in the water samples, illustrating that eDNA can travel long distances as water collects along the river network [Banavar et al., 1999] and aggregates eDNA from the surrounding landscape. Understanding eDNA transport in flowing freshwater is a challenge, and the many factors that affect eDNA transport remain largely unexplored. In this dissertation, we develop a simple conceptual framework to describe eDNA transport in streams and test our model in a laboratory flume.

eDNA is a heterogeneous mixture of particulate organic matter. Large eDNA particles degrade slower than smaller ones: Zhao et al. [2021] and Jo et al. [2019] showed that the polydisperse nature of eDNA influences decay rates. Barnes et al. [2020] showed that the particle size distribution of eDNA influenced its detection, with larger particles easier to isolate on a filter during sampling. The size distribution of eDNA can also influence the perceived concentration during sampling. Shogren et al. [2016] showed that the measured concentration of prepared and homogenized eDNA mixtures could vary by several factors. The inherent variability of observed eDNA data [Jerde et al., 2016] could be associated with other factors such as the streambed substrate for example. eDNA fragments have been associated with turbidity and chlorophyll a, an indication that eDNA is transported adsorbed on other particulates [Barnes et al., 2020]. Larger eDNA particles will settle to the stream bottom faster, while all particles will interact with the substrate eventually, where it could sorb or be filtered. Studies have shown that particles tend to interact with the streambed in the benthic and hyporheic zones where they are temporarily trapped or permanently removed [Aubeneau et al., 2014; Battin et al., 2003]. If there is a legacy amount of eDNA in the sediment, any disturbance such as turbulent bursts and sweeps for example [Roche et al., 2018] could resuspend the particulates and yield samples with exaggerated amounts of eDNA. We suggest that the observed variability in eDNA samples can be explained by its resuspension from the benthic and hyporheic layers where it accumulates. Figure 1 illustrates this conceptual loop of eDNA shedding from a fish and settling to the bottom substrate where it is retained. Resuspension events remobilize the stored eDNA and the suspended particles travel in the water column until they settle out again, continuing to spiral downstream [Stream Solute Workshop, 1992].

The large amount of variability in eDNA data during transport experiments limits our ability to pinpoint its origin. Yet, there is a pressing need to understand eDNA transport in streams to predict its behavior along river networks and the landscape continuum. In the present study, we focus on two questions, i) can we predict the breakthrough behavior of eDNA downstream of its origin? ii) can we identify the sources of variability in eDNA transport data? We conducted three different experiments in an artificial laboratory channel with a coarse sediment bed. We measured (salmon) eDNA retention rates at steady state and measured other transport parameters using a conservative salt. We predicted a priori the eDNA breakthrough behavior and showed good agreement to a measured eDNA breakthrough curve. We replicated the breakthrough experiment after loading the hyporheic zone with eDNA and showed that the data is much more variable if there is a legacy store of eDNA in the streambed.

2. METHODS

2.1 Experimental Setup

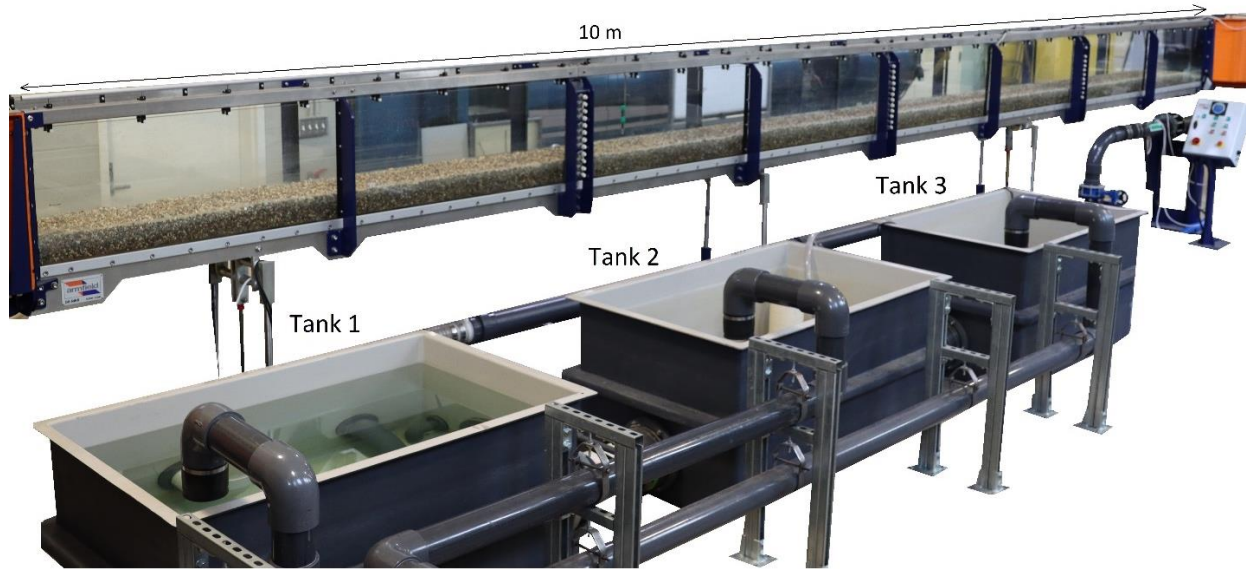


Figure 2. Experimental setup. Picture of the horizontal flume (10 m long; 0.32 m wide) along with the tanks (1000 L each) used for preparing influent solutions. Tank 1 was used to supply clean water, and Tanks 2 and 3 were used for eDNA injections. A 10 cm layer of pea gravel was laid to the flume bed. The flow is from right to left.

All the experiments were carried out in a horizontal flume with a channel of length 10 m, width 0.32 m and 0.45 m depth, pictured in Figure 2 and depicted as a diagram in Figure 3. The flume was connected to three tanks, each having a capacity of approximately 1000 liters. Tank 1 was used to supply clean water to the flume from a 20 000 gal. sump-tank supply (filled with treated well water), and tanks 2 and 3 were used to store and supply the influent solution for the tracer experiments. A half-horse centrifugal pump circulates the water from the tanks to the flume. The flume was used as a flow-through system so that the water did not recirculate and was instead discharged directly to the sewer. Our laboratory channel thus mimics the natural conditions of a real flowing stream. Experiments were performed using two types of tracers, i) sodium chloride as a conservative tracer, and ii) a solution containing the eDNA of Atlantic Salmon (*Salmo Salar*). Before conducting the eDNA experiments the flume characterization was done using sodium chloride to understand its flow dynamics at different discharges as bed conditions. Next, eDNA experiments were performed to estimate retention rates and observe breakthrough curves.

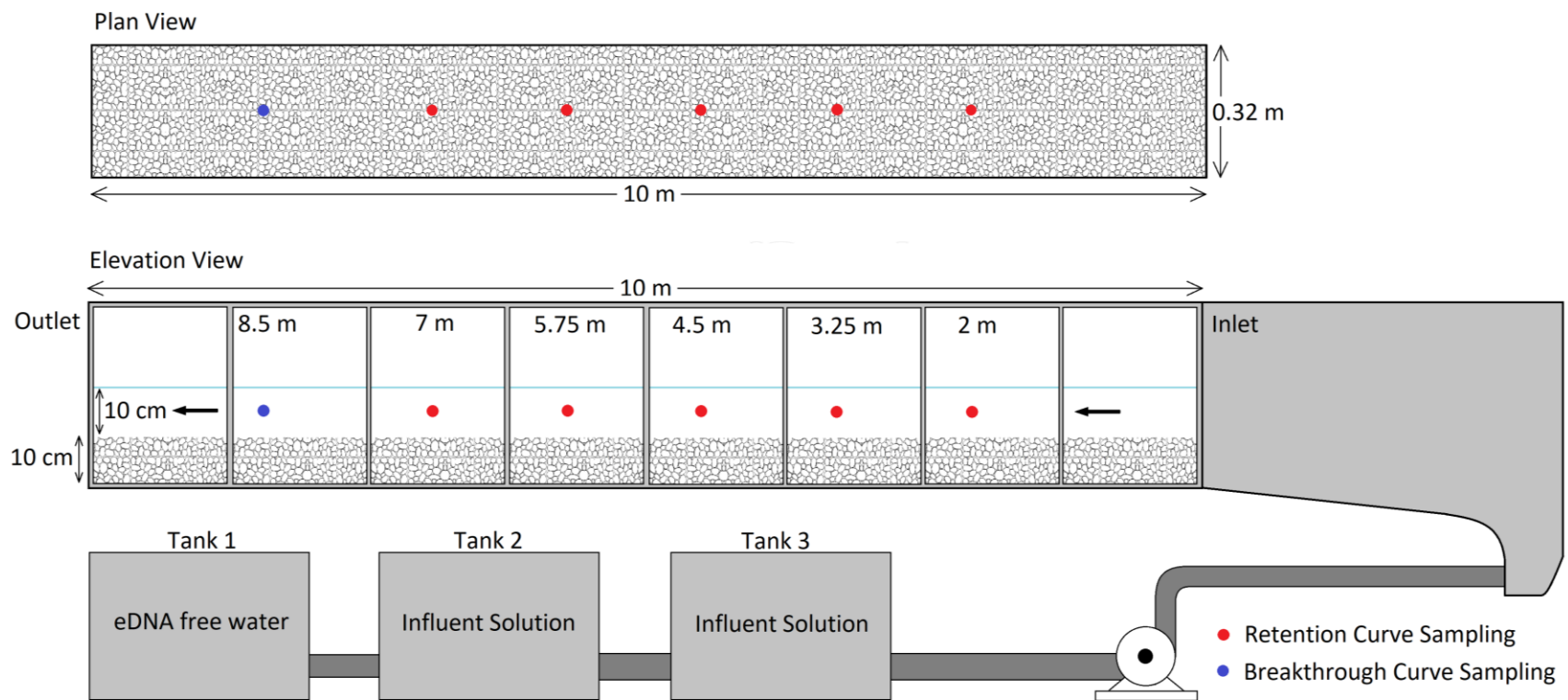


Figure 3. Schematic diagram of the experimental setup.

2.2 Conservative Tracer Experiments

Table 1. Conservative tracer experiment details.

| Experiment No. | Q (L/sec) | S (m/m) | u (m/sec) | Sediment Depth (m) | Flow Depth (m) | Injection Duration (sec) | Salmon Conc. (g/L) | Salt Conc. (g/L) |
|----------------|-----------|---------|-----------|--------------------|----------------|--------------------------|--------------------|------------------|
| BTC_C1 | 1 | 0 | 0.03 | 0 | 0.1 | 720 | 0 | 0.1 |
| BTC_C2 | 3 | 0 | 0.09 | 0 | 0.1 | 240 | 0 | 0.1 |
| BTC_C3 | 5 | 0 | 0.15 | 0 | 0.1 | 144 | 0 | 0.1 |
| BTC_C1_Sed | 1 | 0 | 0.03 | 0.1 | 0.1 | 720 | 0 | 0.1 |
| BTC_C2_Sed | 3 | 0 | 0.09 | 0.1 | 0.1 | 240 | 0 | 0.1 |
| BTC_C3_Sed | 5 | 0 | 0.15 | 0.1 | 0.1 | 144 | 0 | 0.1 |

Experiments were conducted at 1, 3, and 5 liters per second (LPS) discharge with two different bed conditions (with and without sediment). Each experiment was performed thrice to check the reproducibility at varying discharge and bed conditions. The breakthrough curves were measured at 1.5, 5, and 8.5 m from the upstream location. These points were selected to analyze boundary effects (if any) from the inlet and outlet of the flume. The data was collected at a frequency of 10 samples/sec using an Arduino-based setup. The setup consisted of a DF Robot analog electrical conductivity probe connected to an Arduino UNO through a signal conversion board (transmitter). The conductivity probe was mounted approximately at half the height and width of the water column. This was also an attempt to make a low-cost Arduino-based sensor that could be used in field applications for logging conductivity data over a long period at varying frequencies. Before using it for tracer experiments the data from the Arduino setup was compared with the data collected from VWR Conductivity/Temperature meter and a good match was obtained between the two.

The influent solution was made by dissolving 100 g of sodium chloride in 1000 L of tap water in tank 3. To ensure proper mixing of the solution a 0.25 HP utility and dewatering pump was placed inside the tank and was operated throughout the experiment. For each experiment, before the continuous injection, water was pumped from tank 1 for at least 30 minutes through the flume to attain a steady state depth of 10 cm. To achieve this flow depth the tailgate present at the

outlet of the flume was adjusted to an appropriate level. After achieving steady state, the inflow was switched from tank 1 to tank 2 and the influent solution was injected into the flume. During each injection, the background conductivity of tap water and conductivity of the influent solution was noted down from both tanks. For 1,3, and 5 LPS discharge the solution was injected for 720, 240, and 144 seconds respectively and then instantaneously switched back to tank 1, to pump tap water and monitor the falling limb. The falling limb was monitored for 720, 360, and 240 seconds for the three discharges, respectively.

For experiments with sediment, everything remained the same, except, a 10 cm thick layer of pea gravel with a mean diameter of 1 cm was laid down in the flume. The flow depth was kept as 10 cm and the probe was placed at a height of 15 cm from the bottom of the flume. The sediment was washed thoroughly before conducting any experiments to avoid any interference between the conductivity probe and the sand/clay particles which might have come along with the pea gravel.

2.3 eDNA Experiments

Table 2 eDNA experiment details.

| Experiment | Q (L/sec) | S (m/m) | u (m/sec) | Sediment Depth (m) | Flow Depth (m) | Injection Duration (sec) | Salmon Conc. (g/L) | Salt Conc. (g/L) |
|----------------|--------------|------------|--------------|--------------------------|----------------------|--------------------------------|--------------------------|------------------------|
| Retention Rate | 1 | 0 | 0.03 | 0.1 | 0.1 | 1080 | 0.1 | 0.1 |
| BTC_Rep1 | 1 | 0 | 0.03 | 0.1 | 0.1 | 720 | 0.1 | 0.1 |
| BTC_Rep2 | 1 | 0 | 0.03 | 0.1 | 0.1 | 720 | 0.1 | 0.1 |
| BTC_Variance | 1 | 0 | 0.03 | 0.1 | 0.1 | 1080 | 0.1 | 0.1 |

To understand the transport and retention processes of eDNA in coarse sediment beds two types of experiments were designed. All the experiments were performed at a discharge of 1 LPS with a flow depth of 10 cm on a coarse sediment bed comprised of a 10 cm thick layer of pea gravel laid throughout the flume. This particular discharge rate was selected based on a sampling schedule made using the breakthrough curves of the conservative tracer experiments performed previously. It was observed that to monitor both the rising and the falling limb appropriately along with the plateau phase, a discharge rate of 1 LPS would be ideal.

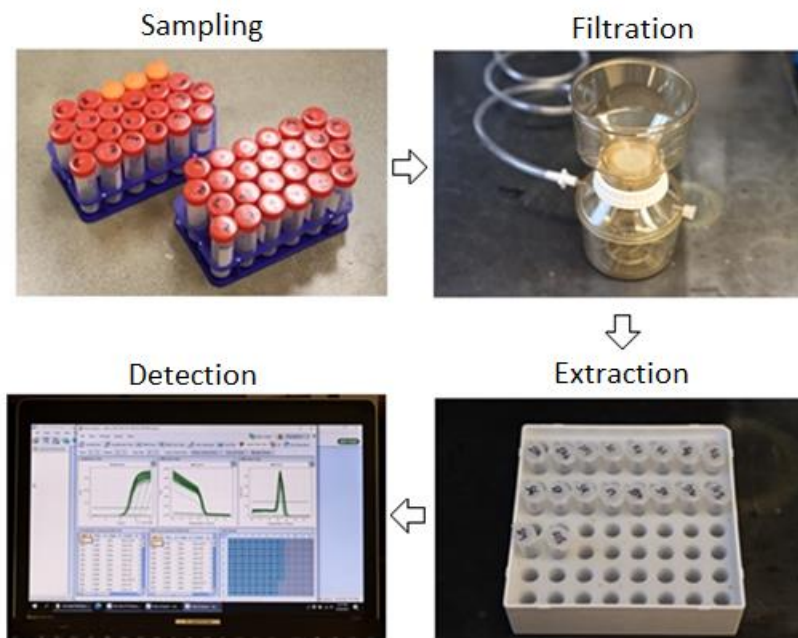


Figure 4. eDNA quantification steps: Sampling, Filtration, Extraction, Detection (clockwise).

2.3.1 Retention Rate

Our first experiment aimed at calculating eDNA retention rates in a coarse sediment bed. The eDNA influent solution (200 g salmon, 2000 L water, and 200 g Sodium Chloride) was prepared in Tank 2 and 3 and the injection was conducted for 1080 seconds. Before the eDNA injection, a solution using 200 g of sodium chloride and 2000 L of tap water was prepared in tank 2 and 3 and tracer tests were conducted to get an estimate of the time it takes for the concentration to be uniform throughout the flume. It was observed that at $t = 820$ sec the concentration reached a uniform value throughout the flume. Prior to the eDNA injection, 3 samples (50 mL each) were collected from the flume to be used as field controls. At $t=820$ seconds, samples were collected at 5 locations (2, 3.25, 4.5, 5.75, 7 m) downstream of the inlet of the flume. At each site, 4 samples were collected at each discharge rate, out of which 3 served as biological triplicates and the fourth one was used to monitor the concentration of the conservative tracer. All the collected samples were stored in a bleach sterilized cooler and filtered within 5 hours of collection.

2.3.2 Breakthrough Curves

In the next experiment, the transport of eDNA was studied using breakthrough curves obtained from continuous injections of an eDNA solution composed of Atlantic Salmon (*Salmo Salar*) DNA. To begin with, the influent solution was prepared by blending a 100 g piece of salmon with 200 mL of tap water for 180 seconds and adding it to 1000 L of tap water in Tank 3. Before adding the salmon solution to the tank, it was filtered through a 0.5 mm mesh to remove any large particles. For proper mixing of the eDNA solution and to avoid settling of particles a 0.25 HP utility and dewatering pump was placed inside the tank and was operated throughout the experiment. 100 g of sodium chloride was also added to the influent solution for comparing the eDNA breakthrough curves with conservative tracer transport and also to account for any dilution that might occur during the injection. Based on previous studies [Shogren et al., 2016], it was assumed that there is no substantial effect of sodium chloride on the eDNA solution.

The eDNA injection was conducted in a similar way as the conservative tracer experiment, 30 mins of tap water from tank 1 to reach steady-state, 720 seconds of eDNA solution from tank 3, and then tap water thereafter. The samples were collected in sterile 50 mL centrifuge tubes at a location 8.5 m downstream from the inlet of the flume. Sampling frequency was decided based on the schedule determined from the conservative breakthrough curves. Time zero ($t = 0$ sec) was designated when the influent solution reached $x = 0$ m. This time was calculated using the conservative tracer breakthrough curves. After the eDNA solution was pumped, samples were collected every 100 sec for the first 300 sec, then at an interval of 50 seconds for the next 1200 sec, and 100-sec intervals thereafter for 400 sec. At each time point two samples were collected, one for measuring the eDNA concentration and the second one for measuring the conductivity. All the eDNA samples were placed in a sterilized cooler and were filtered within 5 hours of collection. Before the pumping of the eDNA solution, 3 samples of tap water were collected from the sampling point to serve as field controls. Three 50 mL samples containing deionized water were also placed in the cooler to account for any contamination that might occur during the extraction process. This experiment was performed twice (BTC_Rep1, BTC_Rep2) to check for reproducibility.

The final experiment was conducted over two consecutive days and was an attempt to monitor a more realistic scenario to reason the large amount of variability observed in eDNA transport experiments. To begin with, 2000 L of influent solution was prepared (Salmon

Concentration = 0.1g/L, Sodium Chloride Concentration = 0.1 g/L) in Tanks 2 and 3, each day. On Day 1, the first injection was conducted, in a way similar to experiment 2 but this time the eDNA solution was injected for 1080 seconds without any monitoring. After the injection, tap water was run for 120 minutes, to completely remove the influent solution and the flume was left idle for rest of the day. On Day 2, tap water was run for 30 minutes followed by 1080 seconds of eDNA solution, and then tap water thereafter. Samples (50 mL) were collected during the second injection at 50 second intervals. The conductivity data was collected parallelly as well. Three samples were collected from Tank 1 (tap water) to serve as field controls. All the collected samples were filtered within 5 hours of collection. The water temperature for all the experiments ranged between 17 to 20° C.

2.3.3 Filtration and Extraction

All the samples were labeled, and vacuum filtered in random order through a 0.2 µm Isopore polycarbonate membrane filter (EMD Millipore Corporation, Billerica, MA, USA). The filters were transferred to sterile micro-centrifuge tubes (MCTs) and stored at -80°C overnight and extracted the following day. The DNA extraction was carried out by following the Qiagen DNeasy method with some slight modifications. The filters were cut in half and submerged in 360 µL of buffer ATL and 40 µL of Proteinase K and vortexed for 15 seconds. The tubes were then incubated at 56°C overnight for approximately 8 hours for the cell lysis to take place. The next morning filters were removed and the MCTs were centrifuged at 6000 rpm for 30 seconds. Next, 400 µL of buffer AL and 400 µL of ethanol were added and vortexed for 15 seconds. The solution was then pipetted into the spin column in two turns and then centrifuged at 6000 rpm for 3 minutes after each turn. After centrifugation, the collection tube, and the flow-through was discarded and a new 2 mL collection tube was attached to the spin column. For removing the contaminants from the DNA, firstly, 500 µL of wash buffers AW1 and AW2 were added and centrifuged for 3 mins at 6000 rpm and 13200 rpm respectively. Finally, the mini-spin column was placed in an MCT, and the DNA was eluted in 120 µL of AE buffer by centrifuging it at 6000 rpm for 3 mins after incubating it at room temperature for 5 mins. The extracted DNA was stored at 4°C before the quantification step. All the DNA samples were quantified within 24 hours of extraction.

2.3.4 DNA Quantification

Table 3. Genus Specific Primers used to amplify *Salmo Salar* DNA

| | Primer | Target Gene | Fragment Size | Annealing Temp. (°C) | Slope | Intercept | Assay Efficiency (%) |
|---------|---|--------------------|----------------------|-----------------------------|--------------|------------------|-----------------------------|
| Forward | 5'– ATCCTGACA GAGCGCGGTT ACAGT – 3' | β-actin | 112 bp | 60 | -3.38 | 28.12 | 97.5 |
| Reverse | 5' – TGCCCATC TCCTGCTCAA AGTCCA – 3' | | | | | | |

All the extracted DNA samples were assayed using previously developed primers (Table 1) [Chalmers et al., 2018]. The primers were tested and validated using the DNA extracted from a tissue of Atlantic Salmon. Amplification because of non-target species was unlikely as all the experiments were performed in controlled conditions with no other species present to contaminate the samples. The primer was synthesized from Integrated DNA Technologies (IDT, Coralville, Iowa) and a 100 µM stock solution was prepared by adding de-ionized water as per instructions by IDT. From the stock solution a 10 µM working solution of both, forward and reverse primer, was made by pipetting 10 µL of primer and adding 90 µL of de-ionized water to it. This working solution was used for all the Quantitative Polymerase Chain Reaction (qPCR). The reactions were set with the following 50 µL mixes: 25 µL of 2×QuantiTect SYBR Green PCR Master Mix (Qiagen, Valencia, CA), 2 µL of each primer (0.4 µM well concentration), 10 µL of template DNA, and 11 µL of sterile water. All the samples were analyzed in triplicates. The following cycling parameters were used: single step at 98°C, followed by 40 cycles at 98°C for 15 seconds, 61°C for 30 seconds, and then 72°C for 30 seconds. All the qPCR runs were performed on a CFX96 Touch Real-Time PCR Detection System in BR White 8-tube PCR strips with ultra-clear caps. For the quantification standard curves, we extracted the DNA from 1 g of salmon by following the steps mentioned before. Serial dilutions were run on each qPCR plate to generate a regression line and calculate the concentration of the unknown DNA samples. In addition to the extracted DNA and the standard

dilutions, each qPCR plate included a negative field control, cooler blank, and a non-template control containing de-ionized water to check for contamination during the qPCR step.

2.4 Transport Modelling

We used two approaches to describe the eDNA transport: an upscaled retention rate based on spiraling concepts (Newbold, Stream solute workshop, 1990), where the overall eDNA transport is considered to conform to a first order removal from the water column, and a simple mobile immobile model commonly known as the transient storage model (TSM) that includes not only removal from the water column, but also from the bed and also considers the net exchange between the surface and the subsurface explicitly. We also demonstrate the correspondence between the two approaches.

2.4.1 Retention Rates

To estimate the retention rates, eDNA concentration data from each sampling location was fitted to a first order equation:

$$\ln C_x = \ln C_0 - k_x x \quad (\text{Eqn. 1})$$

where C_0 is the influent eDNA concentration, C_x is the eDNA concentration at x m downstream from the injection site, and k_x is the per meter retention rate. Before fitting, we corrected the eDNA concentrations using the conservative tracer (salt) data to account for any dilution, but these were minimal in the small reach of the flume. Uptake length (S_w , m), a quantitative transport metric which represents the average distance eDNA travels before being temporarily or permanently retained, was estimated following equation 2.

$$S_w(m) = k_x^{-1} \quad (\text{Eqn. 2})$$

Using the experimental data, we also calculated the depositional velocity, an important retention metric, which can be used for direct comparisons of transport length between streams having varying discharges (Q) by scaling it to larger systems. Depositional velocity is the velocity at which a particle moves from the water column to the benthic zone, and can be calculated using the transport length (S_w):

$$v_d = \frac{Q}{w \cdot S_w} \quad (\text{Eqn. 3})$$

where, v_d = depositional velocity (m/sec)

Q = Discharge (m³/sec)

w = wetted channel width (m)

S_w = uptake length (m)

2.4.2 Transient Storage Model

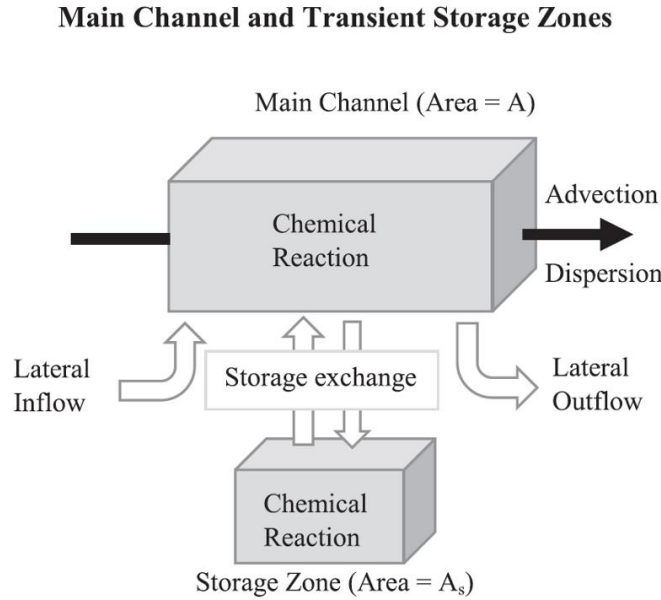


Figure 5 Conceptual representation showing main channel and transient storage zone processes [Runkel and Broshears, 1991]. Calibration parameters in the model include main channel cross-sectional area (A), storage zone area (A_s), storage exchange coefficient (α), and dispersion coefficient (D).

For this study we used a reactive transient storage model (hereby referred to as R-TSM) to estimate the transport parameters for the eDNA breakthrough curves. Transient storage refers to the temporary storage of solutes in water that are moving slowly than the main water body such as hyporheic water [Hauer, F. Richard, and Gary A. Lamberti, eds. *Methods in stream ecology*. Academic Press, 2011.]. The following governing equations (Eq. 4 and 5) (ignoring the lateral flow component), represent the concentration of solute over time in the main channel, and were

used to model the two types of tracers. For modelling the conservative (salt) tracer we ignored the decay term ($-kC$).

$$\frac{\partial C}{\partial t} = -u \frac{\partial C}{\partial x} + D \frac{\partial^2 C}{\partial x^2} + \alpha (C_S - C) - k_m C \quad (\text{Eqn. 4})$$

and

$$\beta \frac{\partial C_S}{\partial t} = -\alpha (C_S - C) - k_{im} C_S \quad (\text{Eqn. 5})$$

where,

C = in-stream solute concentration [mass/m³]

C_S = storage zone solute concentration [mass/m³]

u = average flow velocity (m/s)

D = dispersion coefficient [m²/s]

α = mass transfer rate [/s] (with the inverse expressing a timescale)

β = capacity coefficient representing the ratio of volumes of the immobile zone (sediment bed) to the mobile zone (free stream), sometimes also called A_S/A in TSM formulations (with A = stream channel cross-sectional area [m²] and A_S = storage zone cross-sectional area [m²])

k_m = first order removal rate constant [/sec]

k_{im} = first order removal rate constant in the storage zone [/sec]

We used a Laplace domain solution (Appendix C and D) of the governing equations to estimate the transport parameters of the model. An additional term representing the continuous injection duration was added to the solution.

3. RESULTS

In this section, we describe the results from our experiments. The first subsection will present the results from the retention experiments, including the steady state retention and the predicted and observed breakthrough curves. The second section will show the modeling results and transport parameters and the last subsection will introduce the results from the loading experiments.

3.1 Retention Rate and Breakthrough Curves

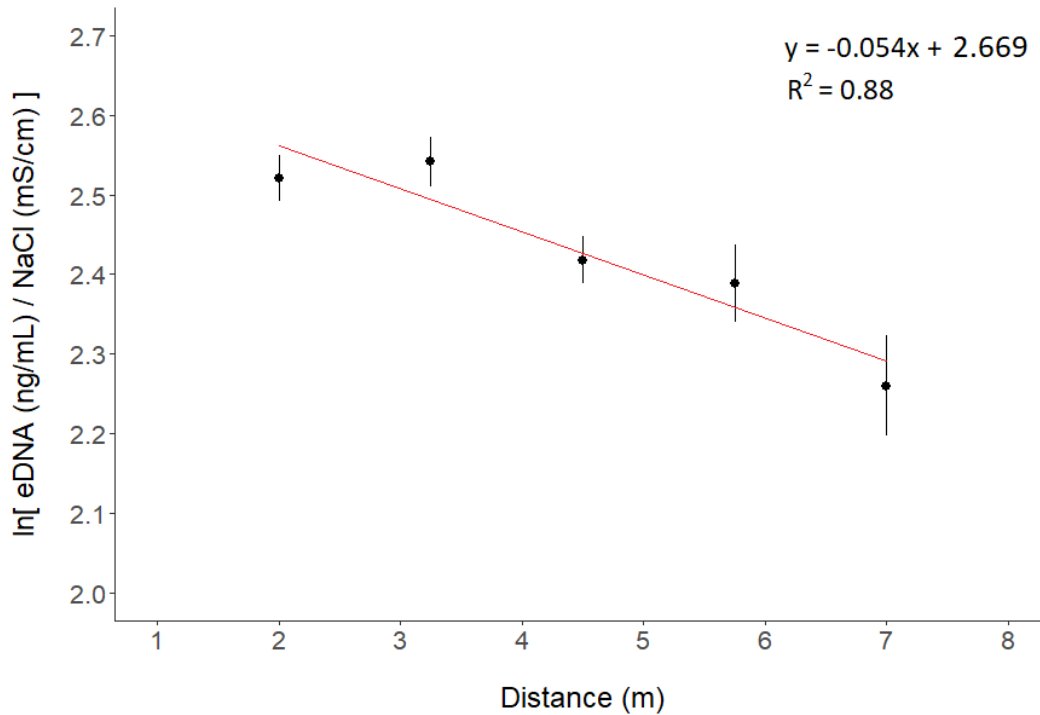


Figure 6. Natural log of eDNA by distance. The solid red line is a regression fit to the data ($N=15$) representing the estimated retention rate ($R^2 = 0.8867$, $p = 0.016$). Each point represents the dilution corrected mean natural log transformed eDNA concentration \pm SE bars ($N = 3$) for each station.

In the first experiment we quantified the downstream decline in eDNA concentrations from the samples collected at the five stations (Figure 6). The retention rate (k_x) corresponds to the slope of the fit in the semi log space (red line in Figure 6). For the pea-gravel sediment bed we used, we

estimated the retention rate at 0.054 ± 0.011 (mean \pm SE, m^{-1}), giving a transport length (S_w) of 18.51 m (15.38 – 23.24 m) ($R^2 = 0.88$, $p = 0.016$). The corresponding eDNA time rate constant is $k_x \cdot u = 0.0015$ /s and the depositional velocity (v_d) was 10.14 mm/min.

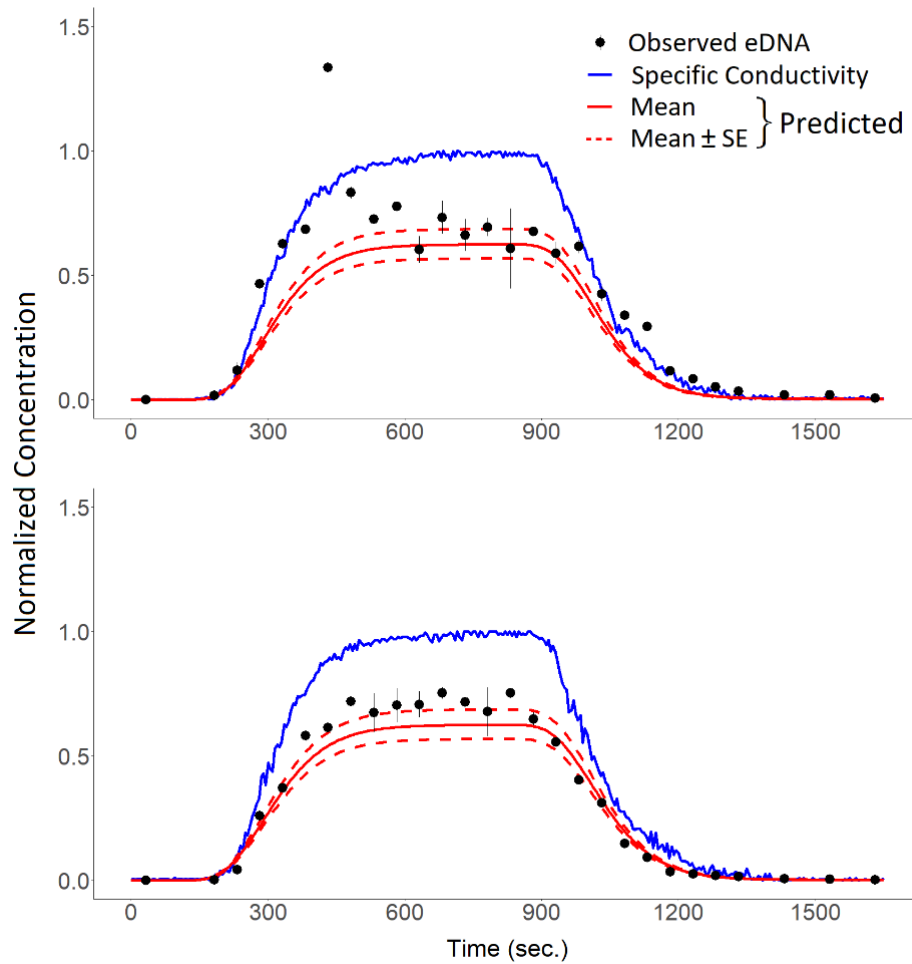


Figure 7. Normalized breakthrough curves of eDNA (observed and predicted) and NaCl solutions through the flume for Experiment BTC_Rep1 and BTC_Rep2.

The breakthrough curves (BTCs) for the conservative tracer (solid blue line in Figure 7) were normalized using the plateau concentration while the eDNA BTCs (black dots in Figure 7) were normalized by the mean influent solution concentration, estimated as 14.43 ng/mL. The eDNA BTC show that part of the eDNA is removed from the water column during transport and settled out of solution, as the plateau never reaches 1. The predicted BTC's were obtained by multiplying the model fitted conservative BTC's by the retention rate (mean \pm SE) and distance at

which the BTC was measured. For the first replicate, the measured data is 1) higher than the predicted data and 2) more variable than the conservative data. For the second replicate, the measured eDNA concentration is slightly higher than the predicted concentrations during the plateau, although the rising and falling limbs were in very good agreement between measured and predicted. Overall, a good match was obtained between the predicted and the observed BTCs, suggesting that the settling and retention of eDNA plays a crucial role in controlling the downstream transport.

3.2 Modeling and Transport Parameters

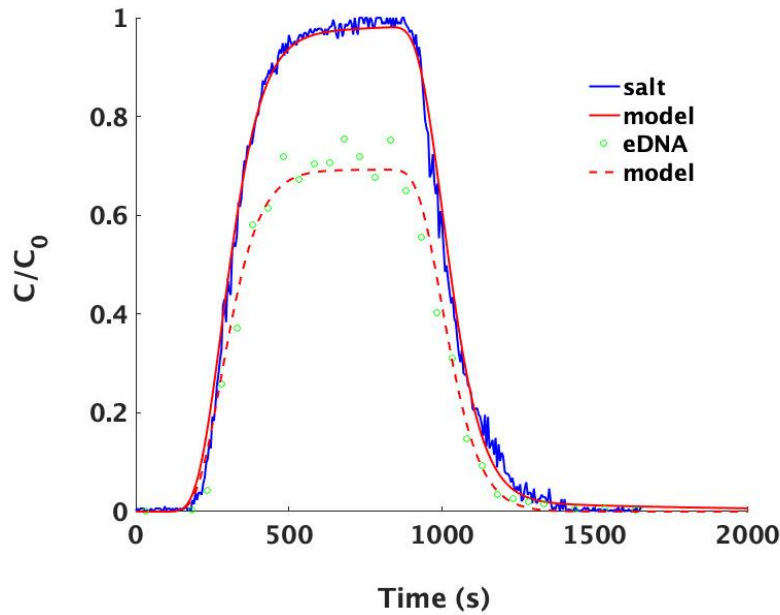


Figure 8. Model results for experiment BTC_Rep2 showing the conservative tracer in blue (salt) and eDNA in green with normalized concentration on the y-axis and time (in seconds) on the x-axis. The solid red line shows the Transient Storage Model fit to the salt and the dashed red line the fit to the eDNA. Model parameter values are given in Table 4.

The normalized specific conductivity was used to estimate the conservative transport parameters while for eDNA, the mean influent solution normalized concentration was used. Figure 8 shows the TSM fits (in red) to the conservative (blue line) and reactive (green dots) tracers for the second replicate. The RMSE and model parameters are reported in table 4. We ran the TSM in two different configurations for the eDNA: a version where all parameters were free (called ‘no

bounds' in table 2), and a version where u , D , α and β were fixed based on the salt fits (called 'bounds' in the table). In all cases, we ran the model with the assumption that there was only first order removal in the water column (column k_t in Table 4). For the second replicate, we also ran a model where both water column and immobile zone first order removal were allowed. The results of this full model are depicted in Figure 9 in a semilog scale to highlight the tailing behavior at late times. In other words, there is a definite exponential release of eDNA from storage after the injection has ended. We also indicate in Table 4 that we could calculate the effective upscaled removal rate from theory (see Appendix C and D), and we are able to match the measured upscaled value of 0.0015 /s. The TSM was able to capture the behavior of both salt and eDNA accurately, but the RMSE is smaller when all parameters are free. In particular, the main difference between the bounded and unbounded fits are in the α parameter, which is almost an order of magnitude higher for the eDNA than for the salt, translating the particulate nature of the eDNA and its settling, thus increasing the exchange timescale between the water column and the bed. The estimated parameters were consistent between the two replicas for both salt and eDNA transport. The velocity is 0.03 m/s. The calculated dispersion coefficient for the experimental conditions is 0.01 m²/sec.

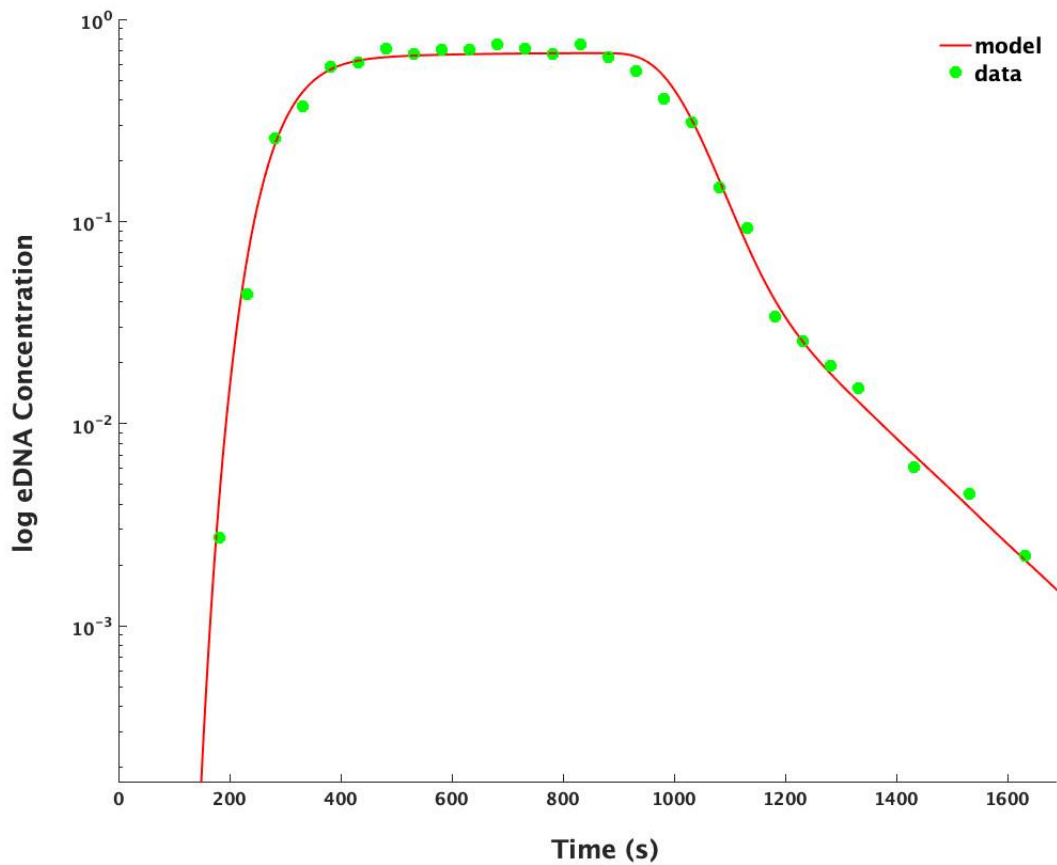


Figure 9 Model fit with a full model with free transient and reactive parameters (only advection and dispersion fixed) for experiment BTC_Rep2. Notice the log scale on the y axis. The eDNA breakthrough curve is represented perfectly by a TSM with reactions in the water column and in the bed. The exchange rate (α) between the stream and the bed is much higher for the particulate than for the solute, a measure of the settling. The reactive parameters k_m and k_{im} represent permanent removal processes (long term sorption, filtration).

Table 4. Estimated transport parameters and root mean square error (RMSE).

| Experiment | u (m/sec) | D (m ² /sec) | α (/sec) | β | k_t ($k_{im} = 0$) (/sec) | k_m (/sec) | k_{im} (/sec) | $k_{eff} = \frac{k_{im}}{1/\beta + \frac{k_{im}}{\alpha}} + k_m$ | RMSE |
|------------------------------|---------------------|-----------------------------------|--------------------------------------|---------------------------|---|-----------------------------------|--------------------------------------|--|-------------|
| BTC_Rep1 (eDNA) No Bounds | 0.0305 | 0.0084 | 0.0062 | 0.1632 | 0.0006 | | | | 0.088 |
| BTC_Rep2 (eDNA) No Bounds | 0.0278 | 0.0052 | 0.0025 | 0.3724 | 0.0012 | $6.8 \cdot 10^{-4}$ | 0.0039 | 0.0015 | 0.033 |
| BTC_Rep1 (eDNA) bounds | 0.0281 | 0.0095 | 0.0003 | 0.3029 | 0.0005 | | | | 0.100 |
| BTC_Rep2 (eDNA) bounds | 0.0281 | 0.0101 | 0.0002 | 0.3255 | 0.0011 | | | | 0.041 |
| BTC_Rep1 (Salt) | 0.0281 | 0.0095 | 0.0003 | 0.3029 | 0 | | | | 0.029 |
| BTC_Rep2 (Salt) | 0.0281 | 0.0101 | 0.0002 | 0.3255 | 0 | | | | 0.025 |

3.3 Variability

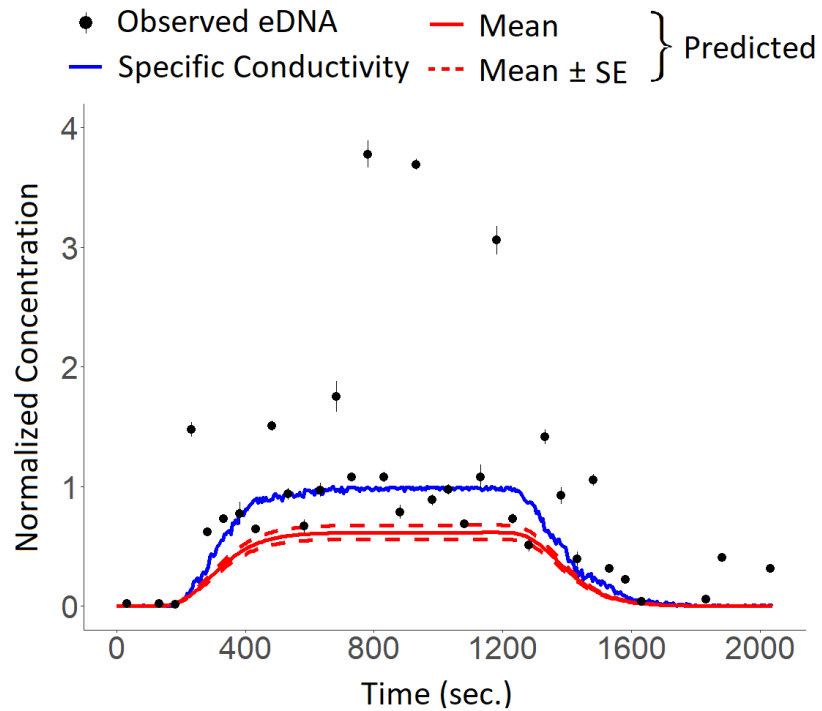


Figure 10. Normalized breakthrough curves of eDNA (observed and predicted) and NaCl solutions through the flume for Experiment BTC_Variance.

In the third experiment, the eDNA breakthrough curves showed a large amount of variability depicting the effect of hyporheic exchange. Even after thoroughly flushing we observed eDNA traces prior to the rising limb and post falling limb region. A significant amount of variability was also observed in the plateau phase with eDNA concentrations reaching almost 4 times that of the influent solution. This noise in the data supports our hypothesis that eDNA accumulation could be occurring in the benthic and hyporheic zones and any disturbances such as turbulent eddies or burst sweeps might push them back in the water column leading to the detection of an exaggerated amount of eDNA.

4. DISCUSSION AND CONCLUSION

One of the key results from this work is that eDNA transport is not conservative in nature and is influenced by retention and settling (Figure 6). In the experiment conducted we successfully quantified significant declines in eDNA concentrations at steady-state and obtained a transport length (S_w) of 18.51 m for eDNA in the pea gravel sediment bed. Even though our numbers when combined with depositional velocity were consistent with previous studies [Jerde et al., 2016; Shogren et al., 2017], some studies [Jane et al., 2014; Deiner et al., 2014; Sansom and Sassoubre, 2017] have also reported highly variable transport distances ranging from a few meters to tens of kilometers. A number of factors can be considered to explain the variation observed in transport lengths, such as, a) eDNA resuspension from the sediment bed to the water column, b) trapping of eDNA in porous media, c) varying discharge rates and stream characteristics. While advection [Nukazawa et al., 2018] and dispersion [Murakami et al., 2019] are the main driving forces behind eDNA transport, our results demonstrate that the stream bottom substrate also plays a crucial role in the retention of eDNA in the benthos zone thereby controlling its transport in lotic environments.

We also obtained overall good matches between the predicted and the observed breakthrough curves. The observed eDNA breakthrough curves were in good agreement with the results obtained from the retention experiment and showed that a part of eDNA was removed from the water column by retention and settling. In the first experiment, a small amount of variability was observed in the eDNA samples, and in both the experiments (particularly in the plateau phase) the measured data was slightly higher than the predicted data indicating that the retention rates could have been overestimated. The possible reason behind this could be the resuspension of eDNA particles [Graf and Rosenberg, 1997]. The high concentration and long persistence of fish eDNA in sediments creates an opportunity for resuspension to influence the temporal and spatial scales of inference from aqueous eDNA [Douville et al., 2007; Leff et al., 1992; Bloesch, 1995]. Jerde et al. [2016], suggests that eDNA is not consistently released from the sediment at a deterministic rate as in case of a conservative tracer but rather at some stochastic time varying rate. We advocate that a better way to estimate retention rates along with the resuspension mechanism could be by sampling at multiple time points so that the temporal variations in the interactions between eDNA particles and the benthos zone could also be captured. Also, it appears that apart from retention, resuspension also has an integral part in eDNA transport and adding a term in

transport models to address resuspension of eDNA back to the water column could lead to more accurate modelling and better predictions.

We also estimated transport parameters for both the conservative tracer and eDNA using a transient storage model. We expected slightly lower retention rates from the transport model as compared to the observed retention rates. For the two breakthrough experiments, we obtained retention rates of 0.02 and 0.04 (m^{-1}). The transport length and the depositional velocity obtained was consistent with the results obtained by Shogren et al. [2017]. The small discrepancy between the two results was because of the variability in eDNA concentrations of the first experiment. The variability in the first experiment was because of the leftover eDNA from the previous experiment. eDNA is adhesive in nature [Barnes et al., 2020] and because if this even after thoroughly flushing the flume there are chances that traces of eDNA are left in the sediment. In order to fix this variability, we thoroughly cleaned the flume with bleach before performing the second experiment. The second breakthrough curve was a good fit to the transient storage model (Figure 8) as compared to the first breakthrough curve and had a comparatively lower RMSE value. Even though a good match was obtained, chances are that the eDNA data collected in natural environments will have much higher variability. In order to capture this high variability and the stochastic [Shogren et al., 2017] and heterogeneous [Klymus et al., 2014] nature of eDNA transport models need further refinement.

In the final experiment, we observed that one of the potential reasons for the large amount of unexplained variability observed in eDNA data is the accumulation of eDNA in the hyporheic zone and its resuspension in the water column thereafter. Turbulent events having sufficient energy might occur occasionally and lead to resuspension of eDNA back into the water column. Turbulent eddies are common in porous media [Anna et al., 2013] and may cause intermittency in particle transport in streams [Singh et al., 2009]. Roche et al. [2018] observed high-frequency concentration fluctuations at the sediment-water interface because of intermittent bursts of flow that drive high concentration pore fluid into the high-momentum free flow. In the present study, we loaded the hyporheic zone with eDNA and then performed a continuous injection to observe the breakthrough curve. The results showed much more variability as compared to the previous data. We believe that this variability is because of the exchange processes in the benthic and hyporheic zones which lead to the addition of eDNA back into the water column. The high energy and high-frequency exchanges lead to erratic increases in eDNA concentration thereby

adding noise to the data. We suggest that numerical efforts can be made to develop a framework in order to quantify this variability and determine the relationship between turbulence and the resulting noise in eDNA data.

Our study is the first to accurately predict downstream eDNA behavior in streams with coarse sediment beds. Our results show that 1) eDNA may not always travel far and can be efficiently removed from the water column in a slow flow shallow water column on coarse sediments, 2) eDNA transport is controlled by retention and resuspension mechanisms, 3) variability in eDNA data could be because of the high energy exchanges at the sediment-water interface. Our study confirms that the nature of eDNA transport is complicated and exhibits multiple levels of complexity. While this study is a step forward in understanding eDNA transport many uncertainties still exist in predicting its source and making inferences about species abundance. We suggest that in order to develop improved transport frameworks, efforts should be made to understand eDNA interactions with the stream bottom substrate as they seem to have a direct impact on eDNA detections. While retention is a major factor affecting eDNA transport there are several other processes such as dilution, sorption, biological degradation, resuspension, and shedding rates which make it difficult to calculate and estimate the species abundance or location by only using eDNA concentration. Having a better understanding of the physical, biological, and ecological mechanisms governing eDNA transport will improve our ability to make inferences about species abundances and locations in a more precise manner. Field sampling efforts also need to be increased as the variability observed in natural environments is likely to be more than controlled laboratory conditions. Moreover, physical, and biological factors affecting eDNA fate and transport need to be incorporated into transport models for making better predictions about the spatial and temporal location of the host organism and help conservationists in better management of species.

REFERENCES

- Ardura, A., Zaiko, A., Martinez, J. L., Samuiloviene, A., Borrell, Y., & Garcia-Vazquez, E. (2015). Environmental DNA evidence of transfer of North Sea molluscs across tropical waters through ballast water. *Journal of Molluscan Studies*, 81(4), 495-501.
- Aubeneau, A. F., Hanrahan, B., Bolster, D., & Tank, J. L. (2014). Substrate size and heterogeneity control anomalous transport in small streams. *Geophysical Research Letters*, 41(23), 8335-8341.
- Banavar, J. R., Maritan, A., & Rinaldo, A. (1999). Size and form in efficient transportation networks. *Nature*, 399(6732), 130-132.
- Barnes, M. A., Chadderton, W. L., Jerde, C. L., Mahon, A. R., Turner, C. R., & Lodge, D. M. (2021). Environmental conditions influence eDNA particle size distribution in aquatic systems. *Environmental DNA*, 3(3), 643-653.
- Battin, T. J., Kaplan, L. A., Newbold, J. D., & Hansen, C. M. (2003). Contributions of microbial biofilms to ecosystem processes in stream mesocosms. *Nature*, 426(6965), 439-442.
- Bloesch, Jurg. "Mechanisms, measurement and importance of sediment resuspension in lakes." *Marine and Freshwater Research* 46, no. 1 (1995): 295-304.
- Bohmann, K., Evans, A., Gilbert, M. T. P., Carvalho, G. R., Creer, S., Knapp, M., ... & De Bruyn, M. (2014). Environmental DNA for wildlife biology and biodiversity monitoring. *Trends in ecology & evolution*, 29(6), 358-367.
- Bothwell, M. L., Lynch, D. R., Wright, H., & Deniseger, J. (2009). On the boots of fishermen: the history of didymo blooms on Vancouver Island, British Columbia. *Fisheries*, 34(8), 382-388.
- Chalmers, L., Vera, L. M., Taylor, J. F., Adams, A., & Migaud, H. (2018). Comparative ploidy response to experimental hydrogen peroxide exposure in Atlantic salmon (*Salmo salar*). *Fish & shellfish immunology*, 81, 354-367.
- De Anna, Pietro, Tanguy Le Borgne, Marco Dentz, Alexandre M. Tartakovsky, Diogo Bolster, and Philippe Davy. "Flow intermittency, dispersion, and correlated continuous time random walks in porous media." *Physical review letters* 110, no. 18 (2013): 184502.
- Deiner, K., Fronhofer, E. A., Mächler, E., Walser, J. C., & Altermatt, F. (2016). Environmental DNA reveals that rivers are conveyor belts of biodiversity information. *Nature communications*, 7(1), 1-9.
- Deiner, Kristy, and Florian Altermatt. "Transport distance of invertebrate environmental DNA in a natural river." *PloS one* 9, no. 2 (2014): e88786.

- Douville, M., F. Gagné, C. Blaise, and C. André. "Occurrence and persistence of *Bacillus thuringiensis* (Bt) and transgenic Bt corn cry1Ab gene from an aquatic environment." *Ecotoxicology and environmental safety* 66, no. 2 (2007): 195-203.
- Graf, Gerhard, and Rutger Rosenberg. "Bioresuspension and biodeposition: a review." *Journal of Marine Systems* 11, no. 3-4 (1997): 269-278.
- Hartvig, I., Kosawang, C., Kjaer, E. D., & Nielsen, L. R. (2021). Detecting rare terrestrial orchids and associated plant communities from soil samples with eDNA methods. *Biodiversity and Conservation*, 1-23.
- Jane, S. F., Wilcox, T. M., McKelvey, K. S., Young, M. K., Schwartz, M. K., Lowe, W. H., ... & Whiteley, A. R. (2015). Distance, flow and PCR inhibition: e DNA dynamics in two headwater streams. *Molecular ecology resources*, 15(1), 216-227.
- Jerde, C. L., Olds, B. P., Shogren, A. J., Andruszkiewicz, E. A., Mahon, A. R., Bolster, D., & Tank, J. L. (2016). Influence of stream bottom substrate on retention and transport of vertebrate environmental DNA. *Environmental science & technology*, 50(16), 8770-8779.
- Jo, T., & Minamoto, T. (2021). Complex interactions between environmental DNA (eDNA) state and water chemistries on eDNA persistence suggested by meta-analyses. *Molecular Ecology Resources*, 21(5), 1490-1503.
- Johnson, M. D., Cox, R. D., & Barnes, M. A. (2019). Analyzing airborne environmental DNA: A comparison of extraction methods, primer type, and trap type on the ability to detect airborne eDNA from terrestrial plant communities. *Environmental DNA*, 1(2), 176-185.
- Kirse, A., Bourlat, S. J., Langen, K., & Fonseca, V. G. (2021). Metabarcoding Malaise traps and soil eDNA reveals seasonal and local arthropod diversity shifts. *Scientific reports*, 11(1), 1-12.
- Klymus, Katy E., Catherine A. Richter, Duane C. Chapman, and Craig Paukert. "Quantification of eDNA shedding rates from invasive bighead carp *Hypophthalmichthys nobilis* and silver carp *Hypophthalmichthys molitrix*." *Biological Conservation* 183 (2015): 77-84.
- Leff, Laura G., J. Vaun McArthur, and Lawrence J. Shimkets. "Information spiraling: movement of bacteria and their genes in streams." *Microbial ecology* 24, no. 1 (1992): 11-24.
- McKelvey, K. S., Young, M. K., Knotek, W. L., Carim, K. J., Wilcox, T. M., Padgett-Stewart, T. M., & Schwartz, M. K. (2016). Sampling large geographic areas for rare species using environmental DNA: a study of bull trout *Salvelinus confluentus* occupancy in western Montana. *Journal of Fish Biology*, 88(3), 1215-1222.
- Mizumoto, H., Urabe, H., Kanbe, T., Fukushima, M., & Araki, H. (2018). Establishing an environmental DNA method to detect and estimate the biomass of Sakhalin taimen, a critically endangered Asian salmonid. *Limnology*, 19(2), 219-227.

- Murakami, Hiroaki, Seokjin Yoon, Akihide Kasai, Toshifumi Minamoto, Satoshi Yamamoto, Masayuki K. Sakata, Tomoya Horiuchi et al. "Dispersion and degradation of environmental DNA from caged fish in a marine environment." *Fisheries science* 85, no. 2 (2019): 327-337.
- Newbold, J. Denis, et al. "Measuring nutrient spiralling in streams." *Canadian Journal of Fisheries and Aquatic Sciences* 38.7 (1981): 860-863.
- Nukazawa, Kei, Yuki Hamasuna, and Yoshihiro Suzuki. "Simulating the advection and degradation of the environmental DNA of common carp along a river." *Environmental Science & Technology* 52, no. 18 (2018): 10562-10570.
- Pfleger, M. O., Rider, S. J., Johnston, C. E., & Janosik, A. M. (2016). Saving the doomed: Using eDNA to aid in detection of rare sturgeon for conservation (Acipenseridae). *Global Ecology and Conservation*, 8, 99-107.
- Roche, K. R., G. Blois, J. L. Best, K. T. Christensen, A. F. Aubeneau, and A. I. Packman. "Turbulence links momentum and solute exchange in coarse-grained streambeds." *Water Resources Research* 54, no. 5 (2018): 3225-3242.
- Sansom, Brandon J., and Lauren M. Sassoubre. "Environmental DNA (eDNA) shedding and decay rates to model freshwater mussel eDNA transport in a river." *Environmental Science & Technology* 51, no. 24 (2017): 14244-14253.
- Shogren, A. J., Tank, J. L., Andruszkiewicz, E. A., Olds, B., Jerde, C., & Bolster, D. (2016). Modelling the transport of environmental DNA through a porous substrate using continuous flow-through column experiments. *Journal of the Royal Society Interface*, 13(119), 20160290.
- Shogren, Ariel J., Jennifer L. Tank, Elizabeth Andruszkiewicz, Brett Olds, Andrew R. Mahon, Christopher L. Jerde, and Diogo Bolster. "Controls on eDNA movement in streams: Transport, retention, and resuspension." *Scientific Reports* 7, no. 1 (2017): 1-11.
- Singh, Arvind, Kurt Fienberg, Douglas J. Jerolmack, Jeffrey Marr, and Efi Foufoula-Georgiou. "Experimental evidence for statistical scaling and intermittency in sediment transport rates." *Journal of Geophysical Research: Earth Surface* 114, no. F1 (2009).
- Stream Solute Workshop. "Concepts and methods for assessing solute dynamics in stream ecosystems." *Journal of the North American Benthological Society* 9.2 (1990): 95-119.
- Takahara, T., Minamoto, T., Yamanaka, H., Doi, H., & Kawabata, Z. I. (2012). Estimation of fish biomass using environmental DNA. *PloS one*, 7(4), e35868.
- Xia, Z., Zhan, A., Gao, Y., Zhang, L., Haffner, G. D., & MacIsaac, H. J. (2018). Early detection of a highly invasive bivalve based on environmental DNA (eDNA). *Biological invasions*, 20(2), 437-447.

Zhao, B., van Bodegom, P. M., & Trimbos, K. (2021). The particle size distribution of environmental DNA varies with species and degradation. *Science of the Total Environment*, 797, 149175.

APPENDIX A. FIGURE AND TABLES

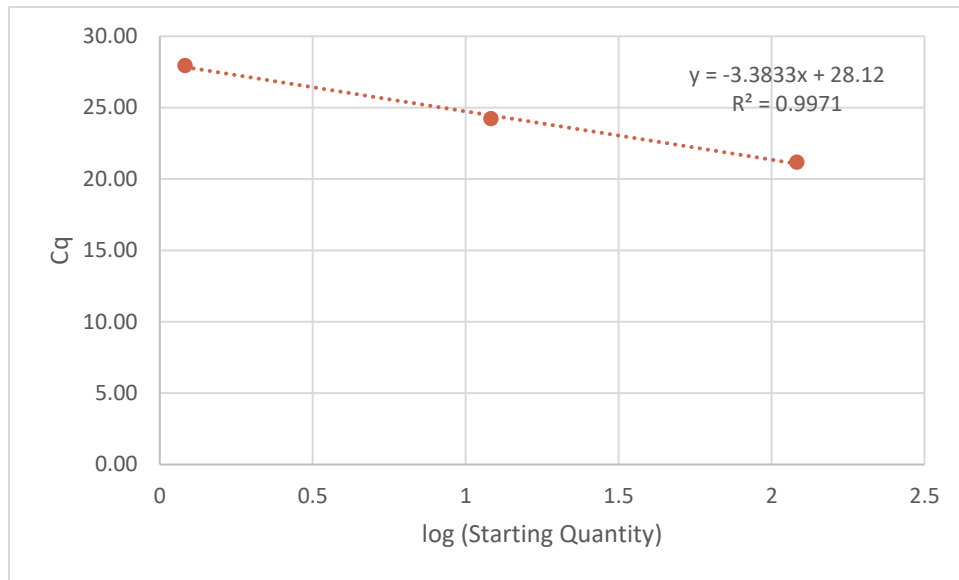


Figure 1A. qPCR standard curve

Table 1A. qPCR standard curve.

| Starting Quantity | log (Starting Quantity) | Average Cq |
|-------------------|-------------------------|------------|
| 121 | 2.0827 | 21.18 |
| 12.1 | 1.0827 | 24.25 |
| 1.21 | 0.0827 | 27.95 |
| | Slope (m) | -3.3832 |
| | Intercept (b) | 28.1195 |
| | Efficiency (%) | 97.5019 |

Table 2A. eDNA retention (Experiment: Retention Rate)

| Sampling Location | ln (eDNA (ng/mL) / NaCl (mS/cm)) | SE |
|-------------------|----------------------------------|--------|
| 2 | 2.5212 | 0.0286 |
| 3.25 | 2.5416 | 0.0313 |
| 4.5 | 2.4181 | 0.0294 |
| 5.75 | 2.3886 | 0.0478 |
| 7 | 2.2601 | 0.0635 |

Table 3A. eDNA concentration (Experiment: BTC_Rep1)

| Time (sec) | Mean Concentration (ng/mL) | Normalized Mean Concentration |
|------------|----------------------------|-------------------------------|
| 32 | 0.0011 | 7.81431E-05 |
| 182 | 0.2477 | 0.0171 |
| 232 | 1.6901 | 0.1171 |
| 282 | 6.7349 | 0.4666 |
| 332 | 9.0333 | 0.6258 |
| 382 | 9.8747 | 0.6841 |
| 432 | 19.2492 | 1.3336 |
| 482 | 12.0000 | 0.8314 |
| 532 | 10.4621 | 0.7248 |
| 582 | 11.2007 | 0.7760 |
| 632 | 8.6966 | 0.6025 |
| 682 | 10.5709 | 0.7324 |
| 732 | 9.5457 | 0.6613 |
| 782 | 10.0000 | 0.6928 |
| 832 | 8.7491 | 0.6061 |
| 882 | 9.7520 | 0.6756 |
| 932 | 8.4976 | 0.5887 |
| 982 | 8.8739 | 0.6148 |
| 1032 | 6.1338 | 0.4249 |
| 1082 | 4.8851 | 0.3384 |
| 1132 | 4.2539 | 0.2947 |
| 1182 | 1.6869 | 0.1168 |
| 1232 | 1.2132 | 0.0840 |
| 1282 | 0.7374 | 0.0510 |
| 1332 | 0.5085 | 0.0352 |
| 1432 | 0.2717 | 0.0188 |
| 1532 | 0.2884 | 0.0199 |
| 1632 | 0.1013 | 0.0070 |

Table 4A. eDNA concentration (Experiment: BTC_Rep2)

| Time (sec) | Mean Concentration (ng/mL) | Normalized Mean Concentration |
|------------|----------------------------|-------------------------------|
| 32 | 0.0010 | 0.0001 |
| 182 | 0.0431 | 0.0030 |
| 232 | 0.6855 | 0.0475 |
| 282 | 4.0820 | 0.2828 |
| 332 | 5.8578 | 0.4059 |
| 382 | 9.1434 | 0.6335 |
| 432 | 9.6682 | 0.6699 |
| 482 | 11.3298 | 0.7850 |
| 532 | 10.5992 | 0.7344 |
| 582 | 11.0795 | 0.7676 |
| 632 | 11.1211 | 0.7705 |
| 682 | 11.8625 | 0.8219 |
| 732 | 11.2994 | 0.7829 |
| 782 | 10.6671 | 0.7391 |
| 832 | 11.8414 | 0.8204 |
| 882 | 10.2187 | 0.7080 |
| 932 | 8.7368 | 0.6053 |
| 982 | 6.3386 | 0.4392 |
| 1032 | 4.8841 | 0.3384 |
| 1082 | 2.3221 | 0.1609 |
| 1132 | 1.4602 | 0.1012 |
| 1182 | 0.5351 | 0.0371 |
| 1232 | 0.4030 | 0.0279 |
| 1282 | 0.3061 | 0.0212 |
| 1332 | 0.2363 | 0.0164 |
| 1432 | 0.0964 | 0.0067 |
| 1532 | 0.0711 | 0.0049 |
| 1632 | 0.0350 | 0.0024 |

Table 5A. eDNA concentration (Experiment: BTC_Variance)

| Time (sec) | Mean Concentration (ng/mL) | Normalized Mean Concentration |
|------------|----------------------------|-------------------------------|
| 32 | 0.3146 | 0.0218 |
| 132 | 0.2659 | 0.0184 |
| 182 | 0.2399 | 0.0166 |
| 232 | 21.3334 | 1.4781 |
| 282 | 8.9231 | 0.6182 |
| 332 | 10.5614 | 0.7317 |
| 382 | 11.1799 | 0.7746 |
| 432 | 9.3054 | 0.6447 |
| 482 | 21.7414 | 1.5063 |
| 532 | 13.5443 | 0.9384 |
| 582 | 9.6569 | 0.6691 |
| 632 | 14.0165 | 0.9711 |
| 682 | 25.2860 | 1.7519 |
| 732 | 15.6035 | 1.0811 |
| 782 | 54.5229 | 3.7776 |
| 832 | 15.5438 | 1.0769 |
| 882 | 11.3636 | 0.7873 |
| 932 | 53.3040 | 3.6932 |
| 982 | 12.8111 | 0.8876 |
| 1032 | 14.0684 | 0.9747 |
| 1082 | 9.9391 | 0.6886 |
| 1132 | 15.6079 | 1.0814 |
| 1182 | 44.1673 | 3.0601 |
| 1232 | 10.5336 | 0.7298 |
| 1282 | 7.3393 | 0.5085 |
| 1332 | 20.4165 | 1.4145 |
| 1382 | 13.3230 | 0.9231 |
| 1432 | 5.6895 | 0.3942 |
| 1482 | 15.2113 | 1.0539 |
| 1532 | 4.5382 | 0.3144 |
| 1582 | 3.2439 | 0.2248 |
| 1632 | 0.5546 | 0.0384 |
| 1682 | -0.8986 | -0.0623 |
| 1732 | -0.2901 | -0.0201 |
| 1782 | -1.0473 | -0.0726 |
| 1832 | 0.8328 | 0.0577 |
| 1882 | 5.8267 | 0.4037 |
| 1932 | -0.5550 | -0.0385 |
| 2032 | 4.5048 | 0.3121 |

APPENDIX B. MATLAB CODES

MATLAB Codes (Provided as Supplement Material)

1. R-TSM Model

Author: Dr. Antoine Aubeneau

2. FMINSEARCHBND

Author: Matlab library, modified Aubeneau

3. INVLAP

Author: Matlab library

APPENDIX C. R-TSM ANALYTICAL SOLUTION

This derivation is similar to Goltz and Roberts (1987), but for a reactive solute. Others have used similar derivations but for different initial or boundary conditions (e.g., McCallum et al., 2020, Kim et al., 2021).

We use a simple reactive transient storage model:

$$\frac{\partial C_m}{\partial t} + \beta \frac{\partial C_{im}}{\partial t} = D \frac{\partial^2 C_m}{\partial x^2} - u \frac{\partial C_m}{\partial x} - k_m C_m \quad (1)$$

$$\beta \frac{\partial C_{im}}{\partial t} = \alpha (C_m - C_{im}) - k_{im} C_{im} \quad (2)$$

where the parameters and variables are as in the main text. The Laplace transform of Equation 2 is:

$$\beta s \bar{C}_{im} - C_{im(0)} = \alpha \bar{C}_m - \alpha \bar{C}_{im} - k_{im} \bar{C}_{im} \quad (3)$$

which leads directly to:

$$\bar{C}_{im} = \frac{\alpha}{\beta s + \alpha + k_{im}} \bar{C}_m, \quad (4)$$

where we assumed that the initial condition in the immobile zone ($C_{im(0)}$) is 0. In equations (3) and (4), s is the Laplace parameter, and the overbar indicates the Laplace transformed variables.

We can replace equation (4) into equation (1) to find its Laplace transform:

$$\begin{aligned} s \bar{C}_m - C_{m(0)} &= D \frac{\partial^2 \bar{C}_m}{\partial x^2} - u \frac{\partial \bar{C}_m}{\partial x} + \alpha \bar{C}_{im} - \alpha \bar{C}_m - k_m \bar{C}_m \\ s \bar{C}_m - C_{m(0)} &= D \frac{\partial^2 \bar{C}_m}{\partial x^2} - u \frac{\partial \bar{C}_m}{\partial x} + \alpha \left[\frac{\alpha}{\beta s + \alpha + k_{im}} \right] \bar{C}_m - \alpha \bar{C}_m - k_m \bar{C}_m \\ \bar{C}_m \left(s + \alpha - \left[\frac{\alpha^2}{\beta s + \alpha + k_{im}} \right] + k_m \right) &= C_{m(0)} + D \frac{\partial^2 \bar{C}_m}{\partial x^2} - u \frac{\partial \bar{C}_m}{\partial x} \end{aligned} \quad (5)$$

With the initial condition a pulse of mass M in the mobile domain, and after Fourier transforming the spatial derivatives to solve and inverting back to the Laplace domain, the solution (i.e., Green's function) is (obtained in Mathematica):

$$\bar{C}_m = \frac{M \exp\left(\frac{Lu}{2d} - \frac{L \sqrt{-\frac{\alpha^2}{\alpha+\beta s+kim} + \alpha + \frac{u^2}{4d} + km + s}}{\sqrt{d}}\right)}{2 \sqrt{d} \sqrt{-\frac{\alpha^2}{\alpha+\beta s+kim} + \alpha + \frac{u^2}{4d} + km + s}}, \quad (6)$$

where L is the distance to the sampling station from the injection. For continuous injections like the ones here, we perform the convolution of the Green's function (equation (6) above) with the initial condition in the Laplace domain (where convolutions are products) for simplicity. The solution cannot be inversed analytically, and we used a numerical inverse Laplace transform function in Matlab that uses the DeHooe algorithm (see codes in the Appendix B).

References:

- Goltz, M. N., & Roberts, P. V. (1987). Using the method of moments to analyze three-dimensional diffusion-limited solute transport from temporal and spatial perspectives. *Water Resources Research*, 23(8), 1575-1585.
- McCallum, J. L., Höhne, A., Schaper, J. L., Shanafield, M., Banks, E. W., Posselt, M., ... & Lewandowski, J. (2020). A numerical stream transport modeling approach including multiple conceptualizations of hyporheic exchange and spatial variability to assess contaminant removal. *Water Resources Research*, 56(3), e2019WR024987.
- Kim, B., Seo, I. W., Kwon, S., Jung, S. H., & Choi, Y. (2021). Modelling one-dimensional reactive transport of toxic contaminants in natural rivers. *Environmental Modelling & Software*, 137, 104971.

APPENDIX D. RELATIONSHIP BETWEEN THE EFFECTIVE REACH-SCALE UPTAKE RATE AND THE ACTUAL REACTION RATE IN THE TRANSIENT ZONE

Here, we demonstrate the relationship between the effective reach-scale uptake rate calculated from traditional solute injections and the actual reaction rate in the transient zone assuming a mobile-immobile transport model. We start with the general Reactive Transient Storage Model (R-TSM), but we ignore the dispersion term for simplicity (i.e., we assume that the spreading of mass is due only to storage processes):

$$\begin{aligned}\frac{\partial C_m}{\partial t} &= -u \frac{\partial C_m}{\partial x} + \alpha \beta (C_{im} - C_m) - k_m C_m \\ \frac{\partial C_{im}}{\partial t} &= \alpha (C_m - C_{im}) - k_{im} C_{im}\end{aligned}$$

where C_m is the concentration in the mobile zone, C_{im} is the concentration in the immobile zone, u is the velocity, β is a capacity coefficient relating the volume of mobile and immobile water, α is the rate of return of water from the immobile zone to the mobile zone, i.e., the inverse of the mean time in storage, k_m is the first order reaction rate in the mobile domain and k_{im} the reaction rate in the quiescent zone. In other versions of the TSM (Bencala 1983), the parameter β is called $\frac{A_s}{A}$, so that α here corresponds to $\alpha \frac{A}{A_s}$ in that version of the model, also referred to as k_2 (Hall Jr et al., 2002), and $\alpha \beta$ here corresponds to α there, also known as k_1 .)

At steady state this gives:

$$\frac{\partial C_m}{\partial t}^0 = -u \frac{\partial C_m}{\partial x} + \alpha \beta (C_{im} - C_m) - k_m C_m \quad (1)$$

$$\frac{\partial C_{im}}{\partial t}^0 = \alpha (C_m - C_{im}) - k_{im} C_{im} \quad (2)$$

and, from Equation 2:

$$C_{im} = \frac{\alpha}{\alpha + k_{im}} C_m \quad (3)$$

so that, replacing in Equation 1:

$$u \frac{\partial C_m}{\partial x} = \frac{\alpha^2 \beta}{\alpha + k_{im}} C_m - \alpha \beta C_m - k_m C_m$$

or

$$\frac{\partial C_m}{\partial x} = -\frac{1}{u} \left(\frac{\alpha \beta k_{im}}{\alpha + k_{im}} + k_m \right) C_m$$

This is a typical first order decay equation with rate (in space)

$$k = \frac{1}{u} \left(\frac{\alpha \beta k_{im}}{\alpha + k_{im}} + k_m \right) \quad (4)$$

Botter et al., (2010) give an equivalent result (but without derivation) for reactions in the immobile zone only. We note the equivalence between k and classic nutrient spiraling metrics: $S_w = 1/k$, where S_w is the so-called uptake length. The equivalent rate in time is

$$k_t = \frac{v_f}{d} = \frac{\alpha \beta k_{im}}{\alpha + k_{im}} + k_m, \quad (5)$$

where v_f is the “uptake velocity”, i.e., a transfer coefficient, and d the depth of the river. The upscaled effective rate (k or k_t) depends both on biogeochemical reaction rates (k_m and k_{im}) and on the hydrologic conductivity between the mobile and immobile zones (α and β), which can unravel transport limitations on measured upscaled biogeochemical rates.

Reference:

Botter, G., Basu, N. B., Zanardo, S., Rao, P. S. C., & Rinaldo, A. (2010). Stochastic modeling of nutrient losses in streams: Interactions of climatic, hydrologic, and biogeochemical controls. *Water Resources Research*, 46(8).